An experimental and kinetic modeling study of cyclopentadiene pyrolysis: First growth of polycyclic aromatic hydrocarbons

Marko R. Djokic [a], Kevin M. Van Geem [a,*], Carlo Cavallotti [b], Alessio Frassoldati [b], Eliseo Ranzi [b], Guy B. Marin [a]

[a] Ghent University, Laboratory for Chemical Technology, Technologiepark 914, B-9052 Gent, Belgium
[b] Dipartimento di Chimica, Materiali e Ingegneria Chimica "G.Natta", Politecnico di Milano, Piazza Leonardo da Vinci 32, 20133 Milano, Italy

Received 24 January 2014
Received in revised form 11 April 2014
Accepted 22 April 2014
Available online 27 May 2014

1. Introduction

Polycyclic aromatic hydrocarbons (PAHs) and soot formation has been and continues to be an area of active research for both pyrolysis and combustion communities because of its scientific and practical importance [1]. PAHs are important intermediates formed during combustion of fuels due to their role in soot formation but even more importantly because of their inherent mutagenic and carcinogenic activities [2]. Among many potential soot precursors' reactions those involving the cyclopentadienyl (CPDyl) radical are considered to be one of the most important contributors to PAHs and soot formation. The CPDyl radical is a resonance-stabilized, ambident, i.e. containing multiple reactive centers, radical that may undergo self-recombination reactions [2,3]. These characteristics make that a significant amount of experimental and theoretical data has been published on the gas phase chemistry involving CPDyl radicals and the corresponding 1,3-cyclopentadiene (CPD) molecule.

In 1950 the thermal decomposition of CPD was studied for the first time by Szwarc [4] in order to determine the bond dissociation energy of CPD into CPDyl radical and hydrogen atom. Although the author anticipated that resonantly stabilized CPDyl radicals would emerge from the reactor and eventually dimerize, a complete cracking of the CPD molecule was observed yielding a decomposition spectra that contained H_2, CH_4, C_2 hydrocarbons, etc. The potential role of cyclopentadienic compounds in the formation of aromatic products was initially postulated by Spielman and Cramers [5] who studied the pyrolytic behavior of phenols and the thermal degradation of CPD. Studies of phenol pyrolysis and phenol hydrogenolysis by Cypres and Bettens [6,7] and by Manion and Louw [8] resulted in the first mechanistic insights into the high temperature chemistry of CPD. Both studies claimed that reactions involving the CPDyl radical and its parent molecule give rise to the formation of naphthalene, indene and methane. Later on, Melius et al. [1] proposed the first mechanism of CPDyl self-recombination to yield naphthalene. The importance of CPDyl moieties in the formation of PAHs was subsequently confirmed by Marinov et al. [9], who investigated the PAHs formation in rich, sooting, premixed methane/ethane flames. This study indicated that PAHs are among

* Corresponding author. Fax: +32 92645824.
E-mail address: Kevin.VanGeem@Ugent.be (K.M. Van Geem).

others formed from CPDyl and fused rings that contain the five-membered CPDyl moiety.

The well-known hydrogen-abstraction carbon-addition (HACA) mechanism, proposed by Frenklach and coworkers [10–12], captures the essence of the sooting process in the postflame region. However, at pyrolysis conditions the HACA mechanism cannot explain entirely the formation and build-up of PAHs [9,13]. Recombination of resonance-stabilized radicals (e.g., propargyl, CPDyl, benzyl) as well as addition reactions between aromatic compounds with six π-electrons and compounds with conjugated double bonds (e.g., acenaphthylene) mainly contribute to the first formation and further growth of PAHs [14–16]. Colket and Seery [17] observed that resonance-stabilized radicals such as CPDyl, benzyl and similar radicals play a relevant role mainly in the pyrolysis region of diffusion flames. This work also indicates that the addition reactions of heavy unsaturated and aromatic species, such as phenyl addition to naphthalene, naphtenyl addition to benzene and similar, may need to be considered.

The growth of PAHs through bimolecular reactions involving heavy radical and non-radical species has recently been the subject of several ab initio simulations based kinetic studies [1,16,18–26]. The aim of these studies was to elucidate the elementary pathways leading to the formation of the smallest PAHs. Because of their high stability, the availability of experimental data, and the relatively limited number of atoms that can be used in high level computational methodologies, naphthalene and indene were the PAHs molecules whose formation mechanisms were mostly investigated. In the present work only those studies that have assessed the role of CPD and/or the CPDyl radical will be discussed. The first quantum chemical analysis about the role of CPDyl moieties in the PAHs formation was performed by Melius et al. [1], using BAC-MP4 and BAC-MP2 methods. The authors have determined the elementary reaction steps that lead to the conversion of two CPDyl radials into naphthalene through the fulvalenyl radical as an intermediate species. The portion of the $C_{10}H_{10}$ Potential Energy Surface (PES) involved in this reaction pathway has been more recently re-examined at a higher level of theory by Kislov and Mebel [23]. It was found that fulvalene is the major product of this reaction mechanism for a large temperature range, thus in partial contradiction with the original proposal. Kern et al. [24] have studied both experimentally and computationally the pyrolytic behavior of CPD in a shock tube setup. Using Rice–Ramsperger–Kassel–Marcus (RRKM) density functional calculations, it has been shown that C–H fission, the initial step in the thermal decomposition of CPD, has a barrier of 351 ± 8 kJ/mol. Further density functional calculations showed that the rate-controlling step in the CPDyl radical decay towards the propargyl radical and acetylene is a 1,2 H-atom shift. Roy et al. [25] have applied PUMP2 level of theory on evaluation of dissociation of the CPDyl radical, as well as its role in PAHs and soot formation. More recently, Wang et al. [16] investigated the reaction between CPD and the CPDyl radical, proposing several mechanisms leading to the formation of indene, naphthalene and benzene. A new reaction pathway was identified that involves the β-scission of a C–C bond from the resonance-stabilized CPD-CPDyl dimer to form naphthalene and benzene. One of these reaction mechanisms was re-examined by Kislov and Mebel [26], who integrated the investigated network of reactions with those found on the $C_{10}H_{10}$ PESs, in an effort to present a unified picture of this complex reaction. More recently new reaction pathways for the reactions of the CPDyl radical and CPD have been proposed by Cavallotti et al. [27]. These authors also estimated channel specific rate constants using ab initio calculations and RRKM/Master Equation theory. One of the conclusions was that the main product is indene. Among the several alternative reaction pathways through which two heavy molecules can react to form naphthalene or indene, the addition of the phenyl radical to butadiene was found to be important by Cavallotti et al. [28] and Ismail et al. [29]. Several other reactions involving benzene and the phenyl radical among the reactants leading to indene formation were studied by Kislov and Mebel [30], reactions involving the cycloheptatrienyl radical [31] or the fulvenallenyl radical [32] as reactants were also found to be important in PAHs formation, as well as the addition of propargyl to the benzyl radical [33].

During the last decade several experimental studies on CPD pyrolysis and oxidation have also been carried out. Butler and Glassman [34] studied the pyrolysis and oxidation of CPD in an adiabatic continuous flow reactor under very diluted conditions (CPD concentrations from 1000 to 3000 ppm by volume in nitrogen carrier gas). They concluded that the recombination and addition (more important at high CPD concentrations) of two C_5 rings to

Table 1
Summary of measured product yields at chosen process conditions at a fixed outlet pressure of 1.7 bara.

	High dilution (24 mol_{N2}/mol_{CPD})					Low dilution (5 mol_{N2}/mol_{CPD})				
Conditions										
CPD flow rate [mg/s]	6	6	6	6	6	27	27	27	27	27
N_2 flow rate [mg/s]	62	62	62	62	62	53	53	53	53	53
T setting [K]	873	973	1023	1073	1123	873	973	1023	1073	1123
Residence time [s]	0.42	0.38	0.36	0.34	0.33	0.42	0.38	0.36	0.34	0.33
Conversion [%]	1.9	7.43	12.18	23.64	65.65	1.97	9.88	22.13	61.71	83.77
Yields [wt%]										
Permanent gasses										
H_2	0.01	0.02	0.10	0.30	1.10	0.02	0.06	0.15	0.82	1.23
CH_4	0.13	0.45	0.66	0.98	2.60	0.07	0.27	0.83	2.70	3.44
Alkenes										
Ethene	0	0	0.14	0.21	0.82	0	0.04	0.23	0.70	1.23
Cyclopentene	1.15	2.2	0.55	0.22	0	0.55	1.24	1.01	0.59	0.06
1,3-CPD	98.1	92.57	87.82	76.36	34.35	98.03	90.12	77.87	38.29	16.23
Aromatics										
Benzene	0	0.48	1.23	2.31	3.85	0	0.28	1.02	4.08	5.39
Toluene	0	0.05	0	0.18	0.73	0	0.06	0.20	0.69	1.38
Xylenes	0	0	0	0.02	0.05	0	0	0.01	0.18	0.10
Styrene	0	0.05	0	0.07	0.49	0	0.07	0.26	0.72	0.92
Indene	0.03	0.96	2.11	3.71	7.85	0.10	1.66	4.71	10.68	9.62
Naphthalene	0.10	0.78	3.36	7.43	20.91	0.09	1.13	4.41	17.31	21.23
Total polyaromatics	0.24	3.28	8.32	18.07	54.18	1.09	6.46	16.32	47.10	68.10

form naphthalene, indene and larger molecules were the major pyrolytic consumption paths of CPD and were also responsible for PAHs and soot formation. The authors used a low grade of only 95% dicyclopentadiene (DCPD) to produce CPD, and hence, the presence of impurities could seriously affect the observed products and their selectivities. Kim et al. [3] studied the aromatic hydrocarbon growth from CPD pyrolysis in a continuous flow reactor at fixed hydrocarbon feed flow rate operating in the temperature range 800–1225 K under very diluted conditions (0.7% molar CPD vapor in nitrogen) starting from 98% + DCPD. The authors chose to condense their reactor effluent and collect it in a dual ice-cooled dichloromethane trap before analysis. The absence of an adequate on-line analysis was one of the reasons that there was significant scatter among the data. Kim et al. [3] observed a crossover of indene and naphthalene yields at ~1050 K, which agrees well with the results of their ab initio work. The indene yield exceeded that of naphthalene at temperatures lower than ~1050 K. Up to ~1200 K naphthalene became the main product while at even higher temperatures benzene became the predominant product. The high yields of the observed products confirmed the importance of the recombination reactions of the CPDyl radicals, as well as the CPDyl radical addition to CPD and heavy unsaturated and aromatic species.

To overcome the lack of accurate pyrolysis data of CPD under mild dilutions we present in this work new experimental data obtained on a dedicated setup at high and low CPD partial pressures in a nitrogen atmosphere. Particular attention is paid to the quantification of minor species which have not been quantified before. These data complement the experimental data of Kim et al. [3] and Butler and Glassman [34], and allow to improve the knowledge on CPD and the CPDyl chemistry. A refined

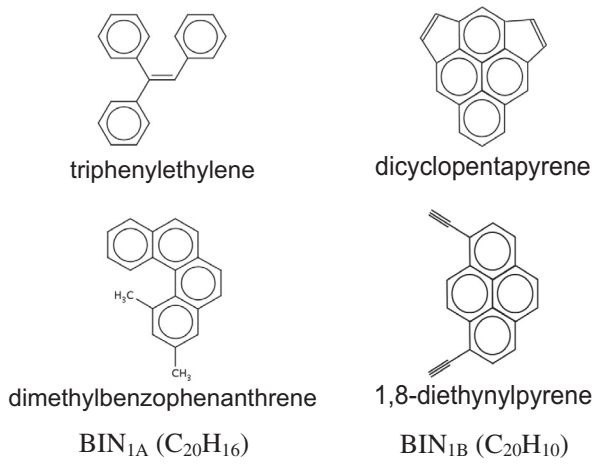

Fig. 1. Reference structures of the two heavy PAHs and lumped species BIN_{1A} ($C_{20}H_{16}$) and BIN_{1B} ($C_{20}H_{10}$), gas phase precursors of soot formation.

Table 2
Main reactions of CPD pyrolysis and aromatic growth.

Reactions		*A*	E · 10^{-3}, kJ/kmol
R 1	$CyC_5H_6 \leftrightarrow CPDyl + H$	1.50E+15	341
R 2	$R + CyC_5H_6 \rightarrow RH + CPDyl$	2 H double allyl type	
R 3	$CPDyl \rightarrow C_2H_2 + C_3H_3$	2.00E+12	285
R 4	$H + CyC_5H_6 \rightarrow C_2H_2 + aC_3H_5$	2.00E+09	33.5
Addition Reactions of CPDyl Radical			
R 5	$CPDyl + CyC_5H_6 \rightarrow C_{10}H_8 + H_2 + H$	3.00E+09	96.3
R 6	$CPDyl + CyC_5H_6 \rightarrow Indene + CH_3$	1.30E+22[a]	96.75
R 7	$CPDyl + CyC_5H_6 \rightarrow Benzene + pC_4H_5$	1.80E+10	107
R 8	$CPDyl + CyC_5H_6 \rightarrow Styrene + C_2H_3$	4.00E+09	107
R 9	$CPDyl + Benzene \rightarrow C_{10}H_8 + CH_3$	3.00E+09	96.3
R10	$CPDyl + Benzene \rightarrow MeNaphthalene + H$	4.00E+08	96.3
R 11	$CPDyl + Toluene \rightarrow Biphenyl + H + H_2$	4.00E+08	80
R 12	$CPDyl + Phenylacetylene \leftrightarrow Fluorene + H$	4.00E+08	80
R 13	$CPDyl + Styrene \rightarrow Fluorene + H + H_2$	1.00E+09	80
R 14	$CPDyl + Xylenes \rightarrow Biphenyl + H_2 + CH_3$	4.00E+08	80
R 15	$CPDyl + EthylBenzene \rightarrow Biphenyl + H_2 + CH_3$	4.00E+08	80
R 16	$CPDyl + Indene \rightarrow Phenanthrene + H + H_2$	4.00E+08	80
R 17	$CPDyl + C_{10}H_8 \rightarrow Phenanthrene + CH_3$	4.00E+08	80
R 18	$CPDyl + C_{12}H_8 \rightarrow 0.5714\ Pyrene + 0.3928625\ BIN_{1A} + H$	4.00E+08	80
R 19	$CPDyl + Biphenyl \rightarrow 0.285714\ Pyrene + 0.57142875\ BIN_{1A} + CH_3$	4.00E+08	80
R 20	$CPDyl + Fluorene \rightarrow 0.14286\ Pyrene + 0.7857125\ BIN_{1A} + H$	4.00E+08	80
R 21	$CPDyl + C_6H_5CH_2C_6H_5 \rightarrow 0.57143\ Pyrene + 0.3928625\ BIN_{1A} + CH_3 + H_2$	4.00E+08	80
R 22	$CPDyl + Phenanthrene \rightarrow 0.42857\ Pyrene + 0.6071375\ BIN_{1A} + H$	4.00E+08	80
R 23	$CPDyl + C_6H_5C_2H_4C_6H_5 \rightarrow 0.14286\ Pyrene + 0.7857125 BIN_{1A} + H_2 + CH_3$	4.00E+08	80
R 24	$CPDyl + Pyrene \rightarrow 0.466667\ BIN_{1B} + 0.58333375\ BIN_{1A} + H$	4.00E+08	80
R 25	$CH_3 + CPDyl \leftrightarrow MeCyC_5H_5$	1.00E+10	12.6
R 26	$C_3H_3 + CPDyl \rightarrow Styrene$	5.00E+09	25
R 27	$CPDyl + CPDyl \rightarrow C_{10}H_8 + H + H$	1.00E+09	25
R 28	$CPDyl + C_6H_5 \rightarrow MeNaphthalene$	2.00E+09	12.6
R 29	$CPDyl + C_7H_7 \rightarrow Biphenyl + H + H$	5.00E+08	25
R 30	$CPDyl + C_7H_7 \rightarrow C_{12}H_8 + H_2 + H + H$	1.00E+09	25
R 31	$CPDyl + RMFEN \rightarrow Biphenyl + H + H$	2.00E+09	12.6
R 32	$CPDyl + RPhenylacetylene \rightarrow Fluorene$	2.00E+09	12.6
R 33	$CPDyl + RStyrene \rightarrow Fluorene + H + H$	2.00E+09	12.6
R 34	$CPDyl + Indenyl \rightarrow Phenanthrene + H + H$	2.00E+09	25
R 35	$CPDyl + C_{10}H_7 \rightarrow 0.5\ Pyrene + 0.5\ Phenanthrene + H + H$	2.00E+09	12.6
R 36	$CPDyl + RBiphenyl \rightarrow Pyrene + CH_3 + H$	2.00E+09	12.6
R 37	$CPDyl + RPhenanthrene \rightarrow 0.5\ BIN_{1B} + 0.5\ Pyrene + CH_3 + H$	2.00E+09	12.6
R 38	$CPDyl + RPyrene \rightarrow BIN_{1B} + CH_3 + H$	2.00E+09	12.6

[a] Rate coefficient of every reaction is expressed as $k = A \cdot \exp(-E/RT)$ except for reaction R6 where a modified Arrhenius equation is used $k = A \cdot T^n \exp(-E/RT)$ for which $n = -3.935$ (Units are m^3, kmol, s, kJ and K).

mechanism for CPD pyrolysis based on earlier work is presented. The mechanism is validated using all three datasets and can be used to describe the evolution of heavy species up to soot particles containing more than 10^6 carbon atoms [35].

2. Experimental

2.1. Pyrolysis setup

The bench-scale pyrolysis setup has been recently discussed in detail [36] and here only differences related to feed/feed section are given. The bench-scale pyrolysis setup consists of three main sections: the feed section, the reactor/furnace section and the product analysis section.

Commercially available dicyclopentadiene (DCPD) (Sigma–Aldrich, 99+% purity) was used as a source of CPD. It was heated to liquid form (307 K) and subsequently fed towards an evaporator kept at 473 K using a coriolis flow meter controlled pump (Bronkhorst, The Netherlands). A temperature of 20 K above the boiling point of DCPD (453 K) is sufficient to gasify DCPD and convert it completely into CPD in-line with the work of Kim et al. [3]. The diluent, N_2 (Air Liquide, Belgium, purity 99.999%), is heated separately to the same temperature. Both the evaporators/heaters and the subsequent mixer are electrically heated and filled with quartz beads, in order to enable a smooth evaporation of the feed and uniform mixing of feed and diluent. The flow rate of the diluent is controlled by a coriolis mass flow controller (Bronkhorst, The Netherlands). For the experiments discussed here dilutions of 5 and 24mol_{N_2}/mol_{CPD} were used, while the temperature was varied from 873 until 1123 K for both dilution regimes, covering a wide CPD conversion range. Information about the experimental conditions under which the pyrolysis of CPD was studied can be found in

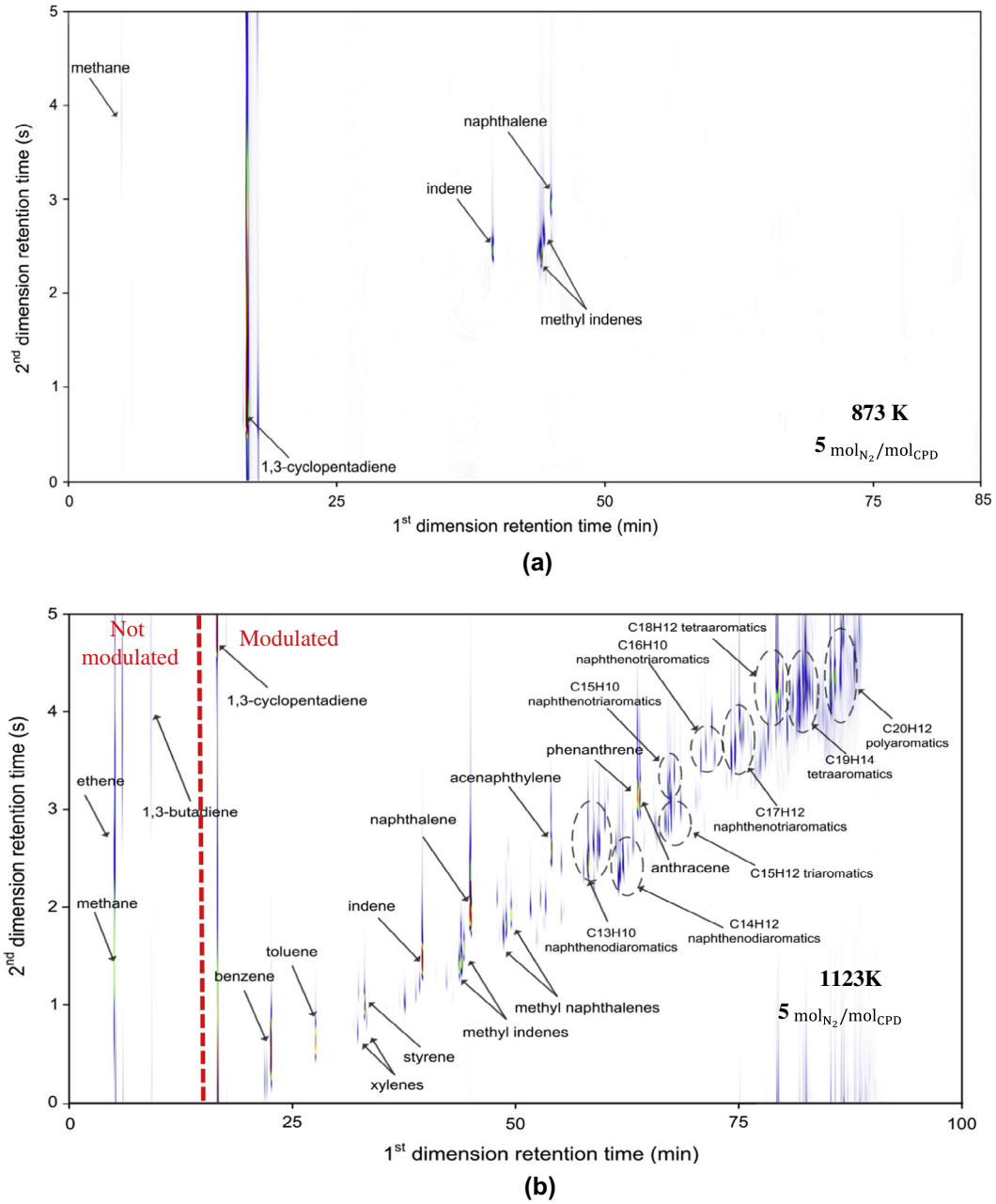

Fig. 2. GC × GC-FID chromatograms of the on-line sampled CPD pyrolysis effluent: (a) T = 873 K, 5mol_{N_2}/mol_{CPD} corresponding to 1.97% CPD conversion and (b) T = 1123 K, 5 mol_{N_2}/mol_{CPD} corresponding to 84% CPD conversion.

Table 1. The flow rates were chosen to obtain a residence time of approximately 300 to 400 ms in both dilution regimes. During changing the reactor temperature profile for both dilutions, the mass flows were kept constant, which resulted in slightly varying of the actual residence time with reactor temperature.

2.2. Product analysis

The analysis section of the pyrolysis set-up has been described at length previously [36–38] and is given in detail in Supplementary Material. The analysis section enables on-line identification and quantification of the entire product stream, from methane to PAHs. Two different gas chromatographs were used for a detailed analysis of the reactor effluent: a so-called refinery gas analyzer (RGA) and a GC × GC-FID/TOF-MS setup (Thermo Scientific, Interscience Belgium). The former is equipped with both an FID and a TEMPUS TOF-MS (Thermo Scientific, Interscience Belgium), enabling both qualitative and quantitative analyses of the entire product stream [36,37]. An overview of the GC × GC–FID/TOF-MS settings used in this work can be found in the Supplementary Material. RGA allows separation and detection of all permanent gases, such as N_2, H_2, present in the effluent, as well as an additional analysis of the lighter hydrocarbons, i.e. C_1–C_4 hydrocarbons.

The tentative identification of compounds is accomplished using two independent orthogonal parameters, Kovats retention indices and the associated mass spectra obtained from GC × GC–TOF-MS analyses. Response factors of all permanent gasses (H_2, CH_4) and light hydrocarbons (C_1–C_4) were determined by means of a gaseous calibration mixture (Air Liquide, Belgium). The response factors of all C_{5+} hydrocarbons were determined using the carbon number concept, relative to methane [39]. For each studied temperature in both dilution regimes, at least 3 repeat analyses were performed on RGA chromatograph which takes approximately one third of the time necessary to complete a GC × GC analysis. Deviations in the obtained results are attributed to uncertainties on the mass flow rates of both feed (CPD) and the internal standard (N_2). In order to calculate the experimental error in the obtained results, replicate experiments for two different temperatures for both dilution regimes were performed. Results of this repeatability study showed relative standard deviations for all detected results less than 10%, with 7% of relative standard deviation for naphthalene being the highest. Subsequently, the component weight fractions were normalized to 100 wt%, in order to enable straightforward interpretation of the obtained results, as well as comparisons with simulated values. In order to assess the significance of the catalytic activity of the reactor wall, a number of experiments were repeated with reactors with different surface to volume ratios, see Supplementary Material. These control experiments showed that the influence of the wall on conversion and product selectivities was negligible.

3. Computational methods

3.1. Reactor models

All the simulations, reaction path and sensitivity analysis were performed with the DSMOKE [40] and OpenSMOKE [41]. The plug flow reactor (PFR) model was employed for modeling the tubular reactor, supplied with the inlet flow compositions, temperature profiles, pressure measurements and reactor dimensions. To gain further insight in the reaction mechanism and the role of certain reaction rate coefficients, a rate of production and sensitivity analyses are carried out for the pyrolysis experiments. The normalized sensitivity coefficients are calculated as follows:

$$\tilde{S}_{ij} = \frac{A_j}{X_i}\frac{\partial X_i}{\partial A_j} = \frac{\partial(\ln X_i)}{\partial(\ln A_j)} \tag{1}$$

in which the effect of the change on the pre-exponential factor A_j of reaction j on the mole fraction X_i of component i is evaluated. Note that the reactions are defined as reversible reactions. The consequence of this is that the equilibrium coefficients are kept fixed while changing the rate coefficients, *i.e.* forward and reverse rates are changed in concert.

3.2. Reaction mechanism construction

The overall kinetic scheme is based on hierarchical modularity and is constituted of more than 400 species involved in over

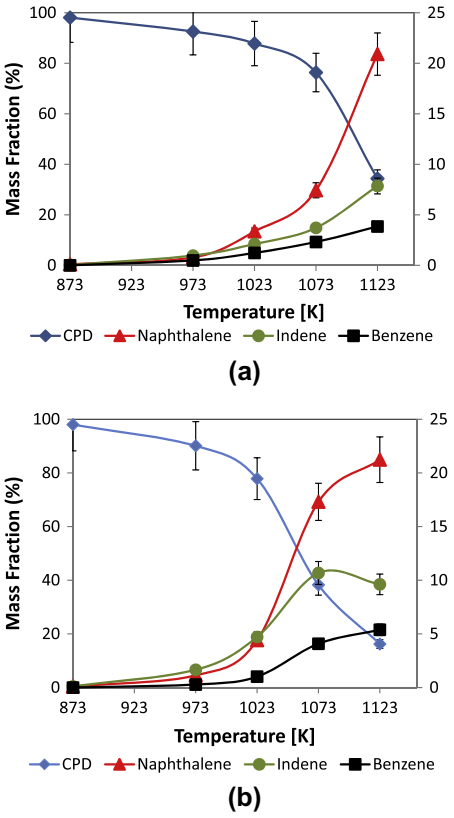

Fig. 3. Normalized (excluding diluent, N2) mass fractions (in %) of CPD and major products (naphthalene, indene and benzene) as a function of temperature for: (a) T = 873–1123 K, $\dot{m}_{CPD}$ = 6 mg/s, $\dot{m}_{N2}$ = 62 mg/s, 24mol$_{N_2}$/mol$_{CPD}$ and (b) T = 873–1123 K, $\dot{m}_{CPD}$ = 27 mg/s, $\dot{m}_{N2}$ = 53 mg/s, 5mol$_{N_2}$/mol$_{CPD}$.

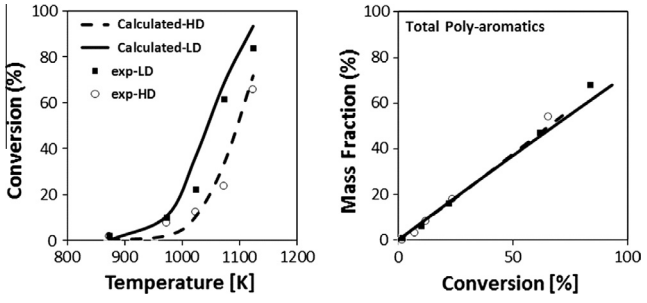

Fig. 4. CPD conversion versus reactor temperature and yields of total Poly-aromatics species versus CPD conversion. LD: low dilution experiments and residence times between 0.42 and 0.33 s (filled symbols and full line), HD: high dilution experiments and residence times between 0.42 and 0.33 s (empty symbols and dashed line).

10,000 reactions [42,43]. The updated and complete POLIMI_1311 mechanism, including thermo and transport properties, is available online at http://www.chem.polimi.it/CRECKModeling/ [44]. The overall kinetic model remains a lumped model, able to analyze in a flexible way also the extension towards heavier PAHs species up soot particles. The model already accounts for the competition between oxidation and pyrolysis reactions. The detailed sub-mechanism of CPD pyrolysis is summarized in Table 2. Units are m^3, kmol, s, kJ and K. Generic hydrogen abstraction reactions on CPD (R2) are derived by using analogy rules [44] and refer to two allyl type H atoms. Particular attention is paid to the successive addition (R5–R24) and recombination reactions (R25–R38) of the CPDyl radical. Further decomposition of smaller radicals and molecules formed starting from CPDyl or CDP originate from the pyrolysis and oxidation mechanism for hydrocarbon fuels up to $C_{16,}$ which is used as seed mechanism.

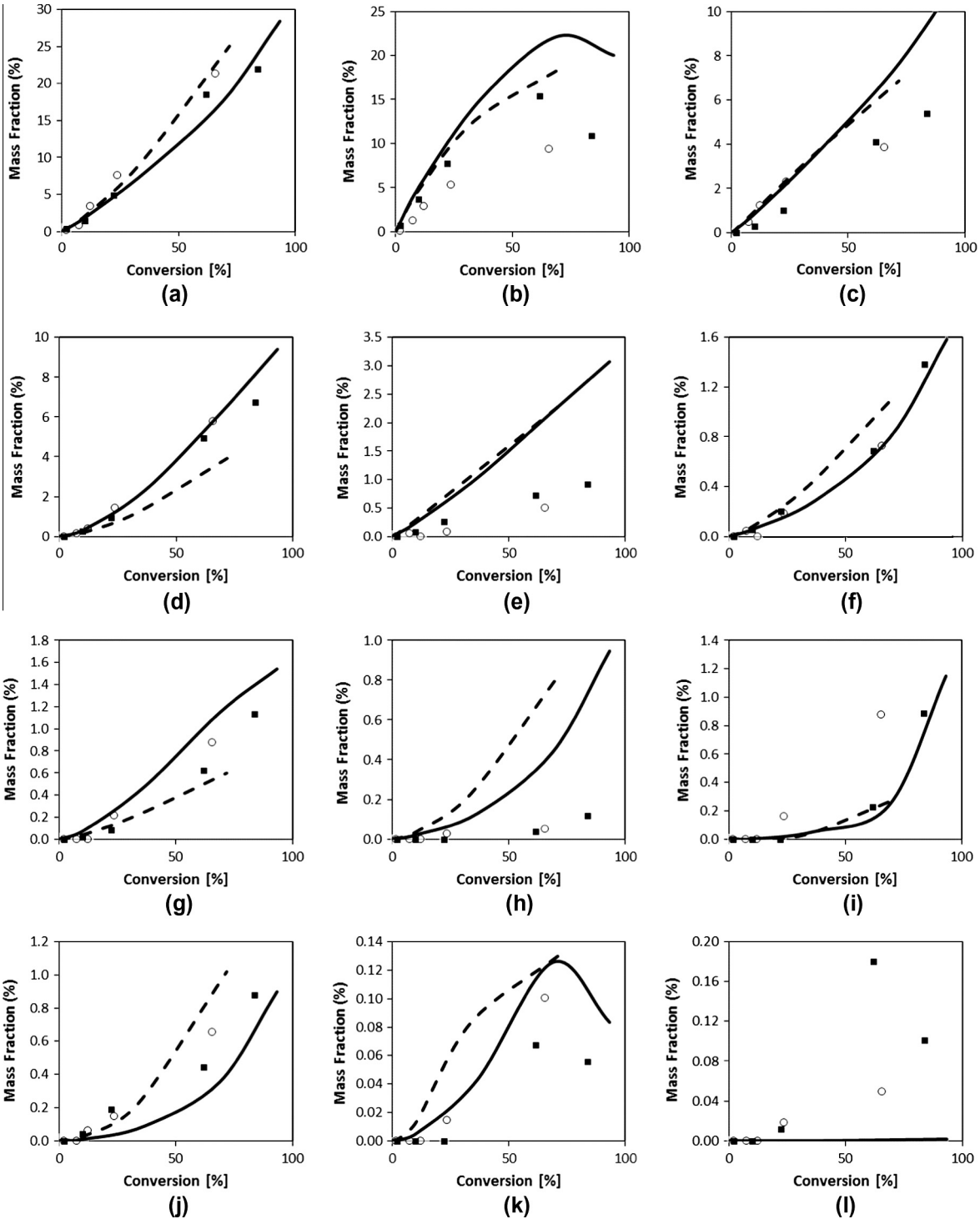

Fig. 5. Yields of major aromatic species versus CPD conversion: (a) naphthalene, (b) indene, (c) benzene, (d) phenanthrene + anthracene, (e) styrene, (f) toluene, (g) fluorine, (h) biphenyl, (i) pyrene, (j) acenaphthylene, (k) phenylacetylene and (l) xylenes. LD: low dilution experiments and residence times between 0.42 and 0.33 s (filled symbols and full line), HD: high dilution experiments and residence times between 0.42 and 0.33 s (empty symbols and dashed line).

3.2.1. Thermodynamic properties and reaction rate coefficients

Thermochemical data for most species were obtained from the CHEMKIN thermodynamic database [45,46]. Unavailable thermodynamic data were estimated using Benson's group additivity method [47,48].

The detailed analysis of CPD and CPDyl radical reactions with the formation of heavy aromatic species contributes to a further identification of the reference reaction rate coefficients of relevant reaction classes of growth of PAHs species. Figure 1 shows some reference structures of the two lumped species BIN_{1A} ($C_{20}H_{16}$) and BIN_{1B} ($C_{20}H_{10}$) [49]. These C_{20} lumped components are the heaviest and terminal species considered in the gas phase kinetic scheme. When the interest moves towards the dynamics and evolution of soot particles, it is also necessary to couple the gas phase kinetic scheme with the model of soot formation. The two C_{20} lumped components become the first precursors of soot species. The soot kinetic model is based on the discrete sectional method: the particles are divided into a limited number of classes covering a mass range from C_{20} up to species containing $\sim 10^6$ carbon atoms; each class or section is represented by two or three lumped species corresponding to the same number of carbon atoms and different H/C ratios, from 0.8 of BIN_{1A} down to values lower than 0.1 for the heaviest lumped species [35]. The reference reaction rate coefficients of the different reaction classes in the soot mechanism are partially derived from the ones identified in the modeling of the PAHs growth from naphthalene to the C_{20} species. The new experimental data on CPD pyrolysis reported here contribute to better identify the reference reaction rate coefficients of recombination and cyclo addition of resonantly stabilized radicals.

3.2.2. Further reaction mechanism refinement

The reference pre-exponential factor for the recombination reactions of large aromatic radicals is set to $5 \cdot 10^9$ [m^3/kmol/s]. This value refers to the recombination of two phenyl radicals to form biphenyl:

$$C_6H_5 + C_6H_5 \rightarrow C_6H_5 - C_6H_5 \quad (2)$$

and agrees well with the pre-exponential factor suggested by Heckmann et al. [50] in their kinetic study on the high-temperature reactions of phenyl radicals. The recombination reaction is considered barrierless. Colket and Seery [17] suggested the same reaction rate coefficients for the recombination reactions of the resonantly stabilized benzyl and CPDyl radicals. Higher values $8 \cdot 10^9 \cdot T^{0.5}$ are suggested by D'Anna et al. [51] in their study on particle nucleation in premixed ethylene flames. According to a recent kinetic modeling work on CPD [27], the selected reaction rate coefficient for the recombination reaction of the CPDyl radicals to form naphthalene (R27 in Table 2) is $1.0 \cdot 10^9 \cdot \exp(-25 \cdot 10^3/RT)$ [m^3/kmol/s]. This activation energy (kJ/mol) is required to overcome the relative stability of the resonant radicals. The same parameters are also assumed for the recombination of the resonantly stabilized benzyl and indenyl radicals. These parameters agree well with the rate coefficient calculated recently by Cavallotti and Polino [52] for the reaction channel leading to the formation of the azulyl radical, a well-known naphthalene precursor: $k = 10^{11.72}T^{-0.853} \cdot \exp(-15.3 \cdot 10^3/RT)$ [m^3/kmol/s]. They also agree with the values proposed by Robinson and Lindstedt [53] $8.53 \cdot 10^{10} \cdot T^{0.246} \cdot \exp(-76.2 \cdot 10^3/RT)$ [m^3/kmol/s] for the recombination of CPDyl radicals. Similar reaction rate coefficients are also used by Slavinskaya et al. [54]. As a generic rule, when more accurate kinetic data are not available, $5 \cdot 10^9$ [m^3/kmol/s] is used for the recombination of aromatic radicals and $1.0 \cdot 10^9 \cdot \exp(-25 \cdot 10^3/RT)$ [m^3/kmol/s] for the recombination of a pair of resonantly stabilized radicals (R30). If a mixed recombination of an aromatic and a resonantly stabilized radical is considered, then a reference reaction rate coefficient of $2 \cdot 10^9 \cdot \exp(-12.6 \cdot 10^3/RT)$ [m^3/kmol/s] is assumed.

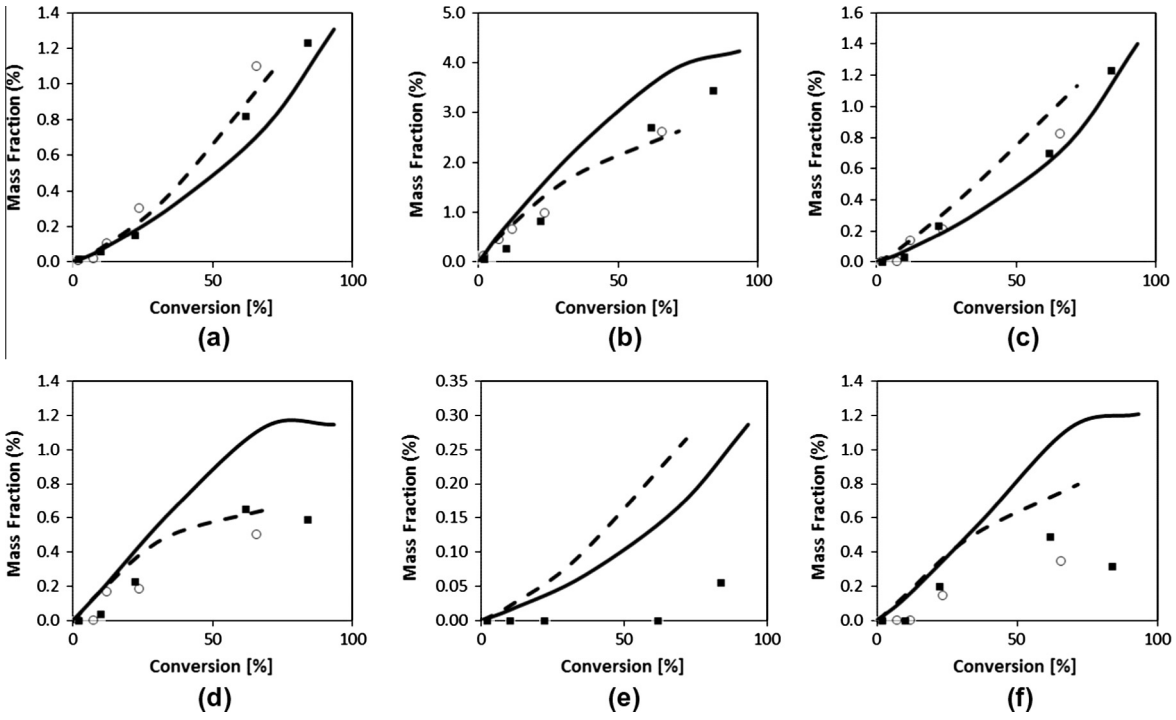

Fig. 6. Yields of light species versus CPD conversion: (a) hydrogen, (b) methane, (c) ethene, (d) propene, (e) propadiene and (f) buta-1,3-diene. LD: low dilution experiments and residence times between 0.42 and 0.33 s (filled symbols and full line), HD: high dilution experiments and residence times between 0.42 and 0.33 s (empty symbols and dashed line).

3.2.3. Addition and cyclo addition reactions of large radicals on aromatic species

Again a distinction between phenyl like and resonantly stabilized radicals is very useful. The selected reference reaction rate coefficients for the addition reaction of aromatic radicals on aromatic species is $1 \cdot 10^9 \exp(-33.5 \cdot 10^3/RT)$ [m^3/kmol/s]. This value reasonably agree with the value $1.1 \cdot 10^{20} \cdot T^{2.92} \cdot \exp(-66.5 \cdot 10^3/RT)$ [m^3/kmol/s] suggested for this reaction class by Apple et al. [55] in their ABF kinetic model of soot formation. This value is also close to the NIST recommended value $4 \cdot 10^8 \exp(-16.75 \cdot 10^3/RT)$ [m^3/kmol/s], suggested by Farh et al. [56] for the biphenyl formation from phenyl and benzene addition:

$$C_6H_5 + \text{Benzene} \rightarrow \text{Biphenyl} + H \quad (3)$$

Reference reactions of the resonantly stabilized radicals can first take advantage from the recent kinetic analysis of CPDyl addition reactions to CPD [27]. Again NIST [57] provides the value $8.4 \cdot 10^8 \exp(-98.2 \cdot 10^3/RT)$ [m^3/kmol/s] for the addition reaction of benzyl radical to benzene, to form diphenyl methane:

$$C_7H_7 + \text{Benzene} \rightarrow \text{Diphenylmethane} + H \quad (4)$$

On these bases, the selected value for the addition and cycloaddition reactions of resonantly stabilized radicals (such as CPDyl, benzyl, indenyl and so on) on aromatic species (R12–R24) is $4 \cdot 10^8 \cdot \exp(-80 \cdot 10^3/RT)$ [m^3/kmol/s].

4. Results and discussion

4.1. CPD pyrolysis

The effect of temperature and dilution on both the CPD conversion and product distribution were studied. Both temperature and dilution have a direct impact on reaction rates, and the effect of these process variables gives important insights into the controlling reactions.

A summary of the measured product yields of the most important species at selected process conditions is given in Table 1. The specific details of all experiments, including information about mass flow rates, are also given in Table 1. Detailed information about product spectra detected at all studied conditions, including temperature profiles in the reaction zone, are available in the Supplementary Material.

Pyrolysis of CPD produces a very complex product spectrum with a strongly varying composition depending on the CPD conversion. Figure 2 shows GC × GC-FID chromatograms of the on-line sampled product obtained at reactor temperatures of 873 (Fig. 2a) and 1023 K (Fig. 2b) for low ($5 mol_{N_2}/mol_{CPD}$) nitrogen dilution. The two dimensional separation is crucial for properly identifying and quantifying the product yields. This is especially true for the formed olefins and PAHs, since these components have similar 1st dimension retention and would therefore remain unresolved using conventional one-dimensional gas chromatography.

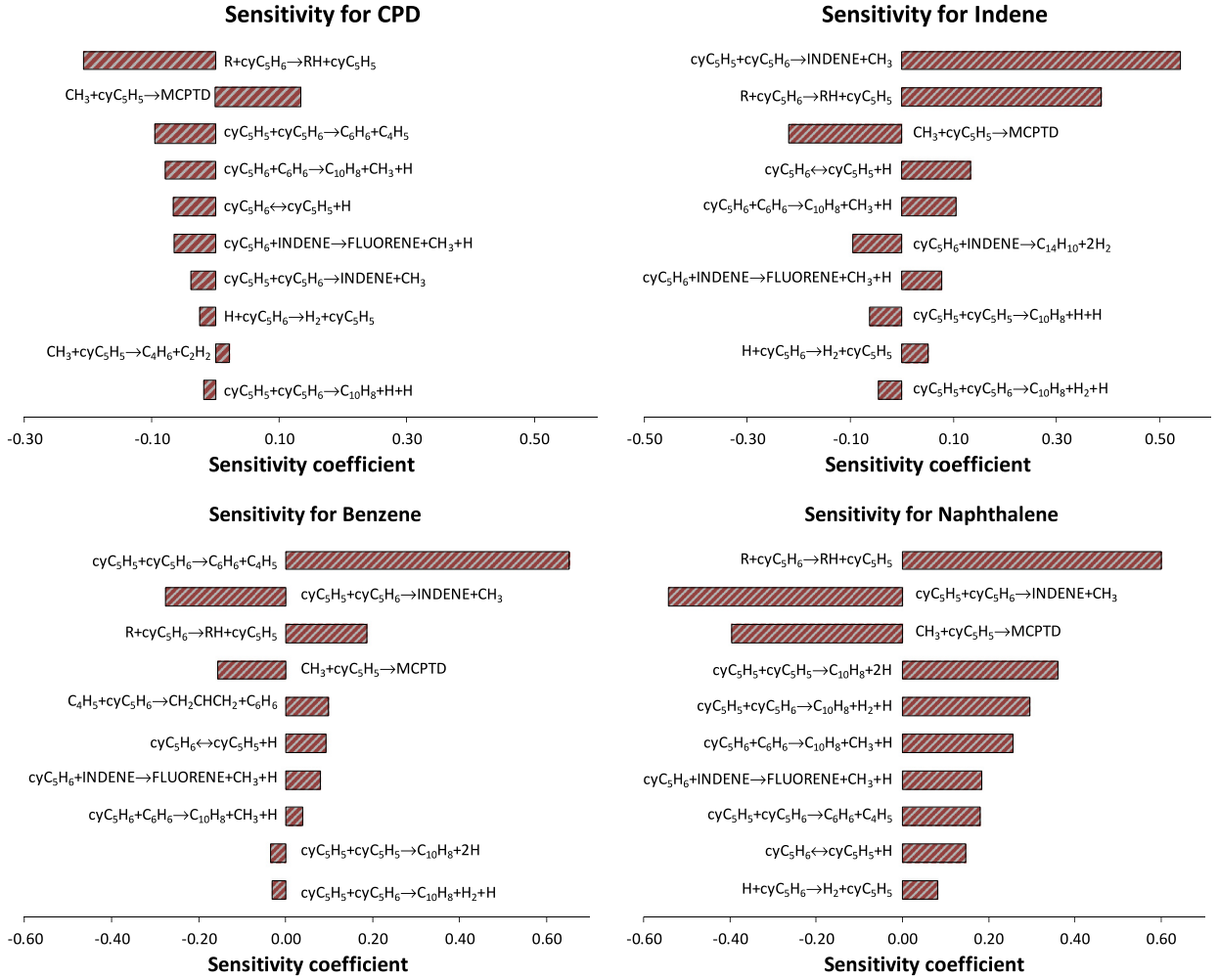

Fig. 7. Sensitivity coefficients for CPD, indene, benzene and naphthalene for the low dilution experiments at 1023 K, 1.7 bara and residence time of 0.36 s.

At 873 K only a small number of pyrolysis products of CPD are detected, such as indene, naphthalene, methyl-indenes, methane. In contrast to the data obtained at 873 K the reactor effluent at 1123 K is significantly more complex, containing on the order of a hundred different compounds. At the most severe conditions, 84% of CPD is converted yielding more than 65 wt% of PAHs with a carbon number up to C_{21}. At higher temperatures more CPD is converted to PAHs. In order to analyze heavier PAHs compounds, the standard PONA (temperature limit at 570 K) column had to be replaced with a high temperature MXT-1 column (See Supplementary Material), which has high maximum operating temperatures of 720 K. This change enabled the analysis of the full product spectrum at even the highest severities (reactor temperature), when PAHs with up to C_{21} were detected.

Both chromatograms clearly indicate that indene, naphthalene and benzene are the main products of CPD pyrolysis over the complete range of CPD conversion. Figure 3 shows the normalized concentration profiles (in wt.%, excluding N_2) of CPD and the main products in the effluent, for both dilutions. At lower temperatures and lower dilution ($5 mol_{N_2}/mol_{CPD}$), indene is the most produced compound, while at temperatures higher than 1023 K, naphthalene exceeds the yields of indene and becomes the major product. Similar trends are observed for the case with higher dilution ($24 mol_{N_2}/mol_{CPD}$). Minor products observed during the pyrolysis of CPD include methane, toluene, styrene, phenanthrene, anthracene, etc.

4.2. Model validation

In order to better analyze the CPD pyrolysis mechanism, the predictions of the kinetic model are compared with three independent sets of pyrolysis experiments:

(i) LCT (UGent) bench-scale pyrolysis tubular reactor (present work)
(ii) Princeton's adiabatic, atmospheric continuous flow reactor (Butler and Glassman [34])
(iii) Georgia Tech continuous flow quartz tubular reactor (Kim et al. [3])

Moreover, to further validate the kinetic model also at combustion conditions a fourth comparison refers to the laminar flame speeds of cyclopentadiene/air mixture recently determined by Ji et al. [58].

4.2.1. LCT (UGent) bench-scale pyrolysis tubular reactor

The complete detail of experimental measurements is reported in the Supplementary Material. Due to the semi-detailed nature of the kinetic scheme, several heavy species are grouped into a reduced number of lumped species. Figures 4–6 report the complete comparisons between experimental data and model predictions.

Figure 4 shows that the kinetic model properly predicts the higher CPD conversion in the low dilution experiments, due to the apparent reaction order of CPD decomposition higher than one. Moreover, Fig. 4 also shows that the mass yields of PAHs (C9 + components) reach ~70% at the highest conversions. Also in this case the model properly agrees with experiments and confirm a similar behavior for both dilution regimes. Yields of major aromatic and light species versus CPD conversion are reported in Figs. 5 and 6, respectively.

Naphthalene, indene and benzene are the major products and their selectivity is not significantly affected by the different dilution. Their production rate is mainly due to the CPDyl radical

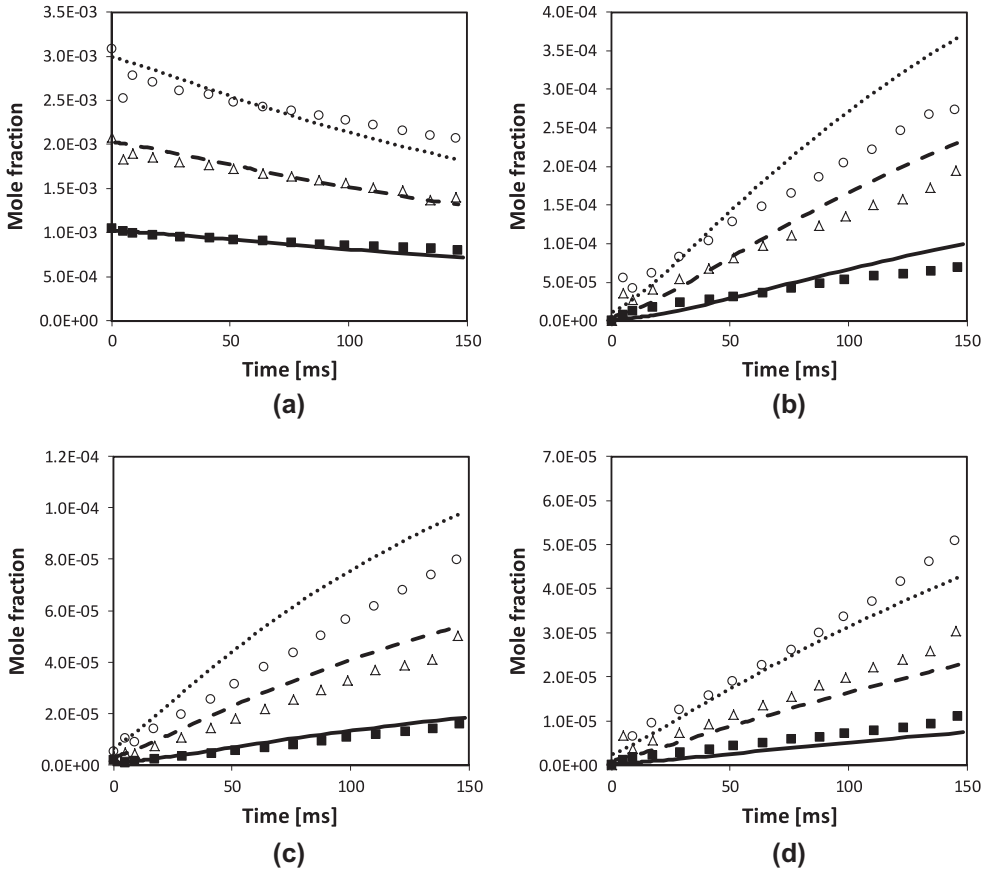

Fig. 8. Effect of CPD concentration on mole fractions of: (a) CPD, (b) naphthalene, (c) indene and (d) benzene. Symbols: experimental Runs 8 (triangles, $\varphi = 100$, $T_0 = 1147$ K, $[CPD]_0 = 2083$ ppmv), 9 (squares, $\varphi = 44.4$, $T_0 = 1148$ K, $[CPD]_0 = 1044$ ppmv) and 10 (circles, $\varphi = 143$, $T_0 = 1147$ K, $[CPD]_0 = 3081$ ppmv) [34]. Lines: model predictions.

addition reactions to CPD, together with the self-recombination reaction of CPDyl radicals. The sensitivity analysis will be further discussed in the next paragraph.

Figure 7 shows the sensitivity analysis for the low dilution experiment at 1023 K. CPD conversion is mainly controlled by the H-abstractions as well as by the chain initiation reaction. The CPDyl radical addition reactions on CPD mainly govern the selectivity to form the major products, namely naphthalene, indene, and benzene. Self-recombination reaction of CPDyl radicals is a relevant source of naphthalene. CPDyl and methyl radical recombination reaction to form methyl-cyclopentadiene reduces the CPD conversion, for this reason it has a negative sensitivity coefficient also for indene and benzene formation. Sensitivity analysis clearly highlights the role of indene as an important intermediate towards the formation of heavier species.

4.2.2. Princeton's adiabatic atmospheric continuous flow reactor [34]

Butler and Glassman [34] analyzed CPD reactivity in several pyrolysis and oxidation conditions by varying the concentration, equivalence ratio, and initial temperature in the Princeton flow reactor. At all conditions, the growth of the molecular mass confirms the significant role of recombination and condensation

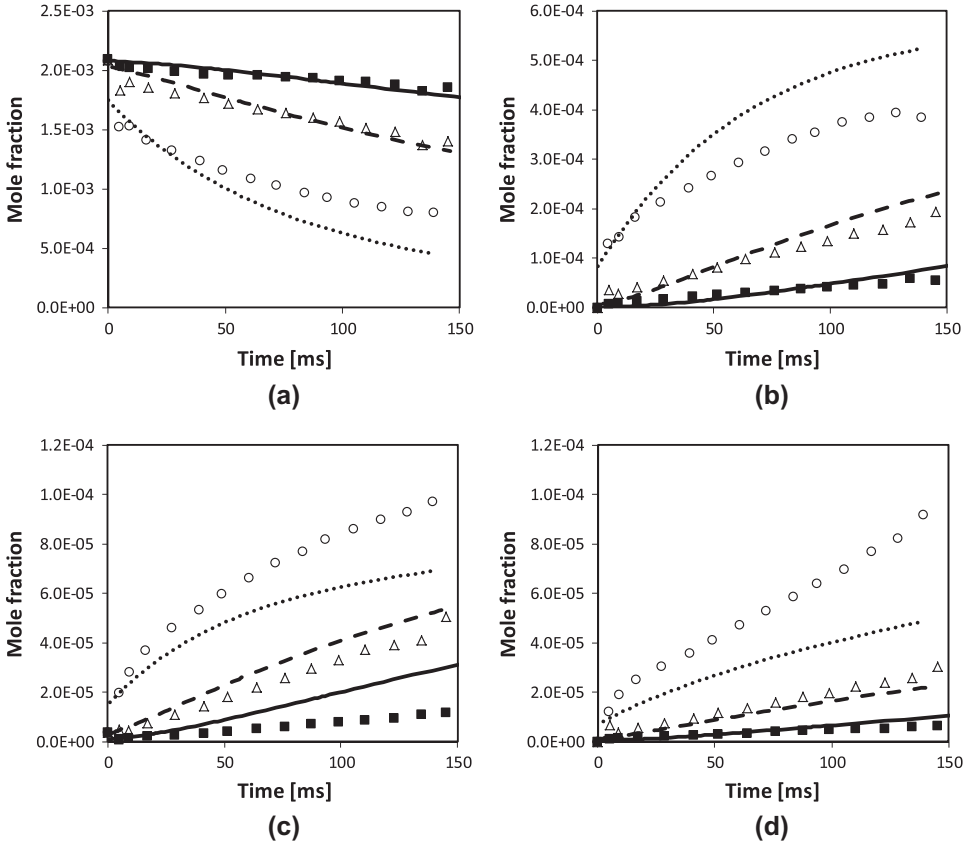

Fig. 9. Effect of Temperature (1100–1200 K) on mole fraction of: (a) CPD, (b) naphthalene, (c) indene and (e) benzene. Symbols: experimental Runs 8 (triangles, $\varphi = 100$, $T_0 = 1147$ K, $[CPD]_0 = 2083$ ppmv), 11 (squares, $\varphi = 98.6$, $T_0 = 1106$ K, $[CPD]_0 = 2094$ ppmv) and 12 (circles, $\varphi = 97.8$, $T_0 = 1202$ K, $[CPD]_0 = 2077$ ppmv) [34]. Lines: model predictions.

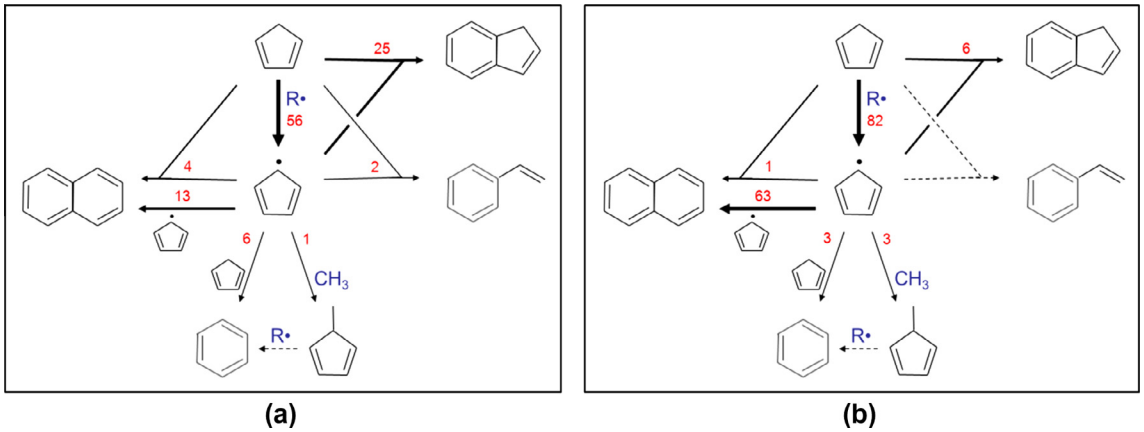

Fig. 10. Reaction path analysis at 50% CPD conversion: (a) Ghent flow reactor (1023 K, 1.7 atm, 0.36 s) and (b) Princeton flow reactor (1203 K, 1. atm, 0.06 s). Thickness of the arrows reflects the relative importance of the different reaction paths.

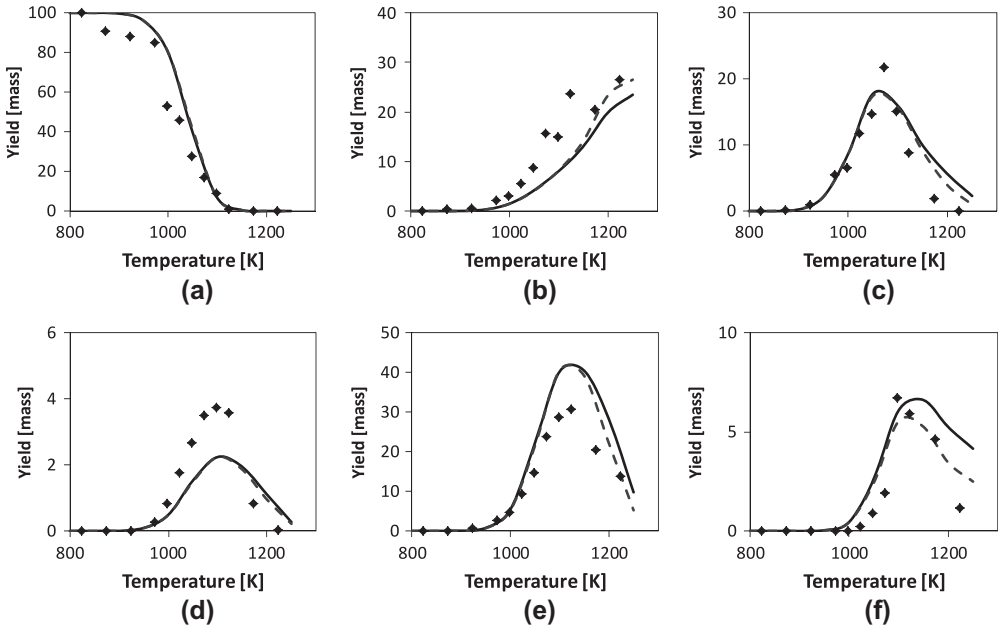

Fig. 11. CPD conversion and yields of major aromatic products versus reactor temperature. Comparison of experimental (diamonds) and predicted values (lines): (a) CPD, (b) benzene, (c) indene, (d) styrene, (e) naphthalene and (f) $C_{14}H_{10}$s [3] Dashed lines are model predictions including the soot kinetic model. [35].

reactions of CPDyl and indenyl radicals. Figures 8 and 9 compare experimental measurements and model predictions in pyrolysis conditions (Runs 8–12), confirming the reasonably accurate model predictions, both in respect of CPD concentration and temperature effect. Note that, following usual practice employed for comparison with Princeton flow reactor data, predicted mole fraction profiles are shifted by 20 ms in order to match the fuel conversion [59]. Further detailed comparisons between experimental measurements and model predictions, both in pyrolysis and oxidation conditions are reported in the work of Cavallotti et al. [27].

Figure 10 compares the reaction path analyses in the operating conditions of Ghent and Princeton, at ~50% CPD conversion. Thickness of the arrows reflects the relative importance of the different reaction paths. The lower temperature conditions of Ghent experiments emphasize the role of CPDyl radical addition reactions on CPD, while the higher temperatures increase the importance of H abstraction reactions, thus favoring CPDyl radical and successive recombination reaction to form naphthalene. For this reason, naphthalene formation prevails at the high temperatures, while indene is the prevailing product at lower temperatures.

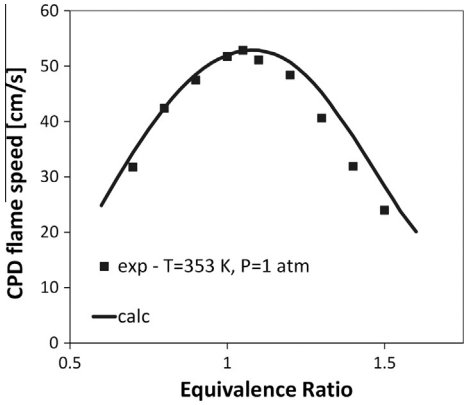

Fig. 12. Premixed laminar flame speed of CPD/air mixtures at atmospheric pressure and initial temperature of 353 K. Full line: model prediction. Experimental data (square symbols) are taken from the work of Ji et al. [58].

4.2.3. Georgia Tech continuous flow quartz tubular reactor [3]

Kim et al. [3] studied the pyrolysis of CPD from 800 K up to 1200 K in a laminar flow reactor, 48 cm long and 1.7 cm in diameter, at a nominal residence time of 3 s. Nitrogen was used as a carrier gas, and the gas stream entering the reactor consisted of N_2 with 0.7% molar CPD. The gas temperature in the reaction zone was nearly uniform both in axial and radial directions. Due to the large contact times, these experimental data highlight the pyrolytic growth of PAHs via CPDyl radical recombination and addition reactions. Again, benzene, indene, and naphthalene were the major pyrolysis products. Figure 11 shows the good agreement between experimental measurements and model predictions versus the reactor temperature. The formation of naphthalene, indene, and styrene are correctly predicted by the kinetic model with a proper location of the maximum. Note that these deviations seem the opposite with respect to the experimental data of Fig. 5. Mainly indene and phenantrene profiles underline the importance of their successive reactions involving CPDyl and indenyl radicals as well

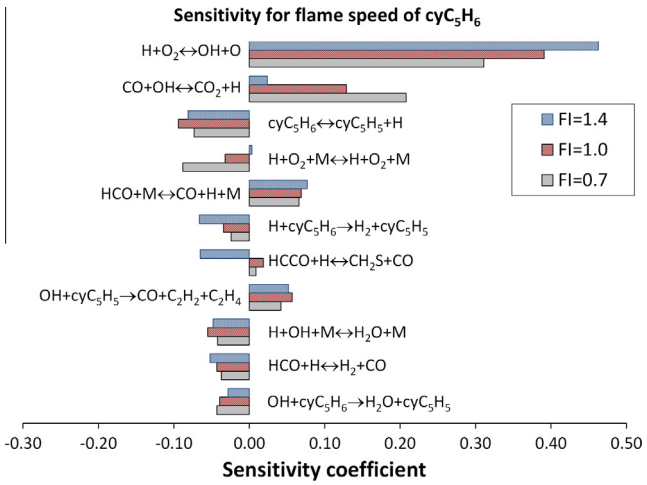

Fig. 13. Sensitivity analysis for CPD flame speed at atmospheric pressure, initial temperature of 353 K and different the fuel–air equivalence ratios.

as heavy molecules and radicals. The predicted carbon selectivity towards pyrene, and heavier species becomes ~30% at 1200 K, while it surpasses 50% at 1250 K. These experimental data highlight the role of the successive growth and condensation of aromatic species, thus allowing a better identification of the reaction rate coefficients of the corresponding elementary and/or lumped reactions. Figure 11 also shows the importance of the successive reactions involved in the soot formation process. Dashed lines show that the yield of aromatic species, but benzene, slightly decreases due to the presence of these successive reactions.

4.2.4. Premixed laminar flame speed

Laminar flame speeds of cyclopentadiene/air mixture were recently determined by Ji et al. [58] in a counterflow configuration at atmospheric pressure and for a wide range of equivalence ratios. Figure 12 shows the good agreement between experimental and predicted laminar flame speeds of cyclopentadiene/air flames at $T_0 = 353$ K and $p = 1$ atm. The sensitivity analyses reported in Fig. 13 compare the coefficients in lean, stoichiometric, and rich flame conditions and they reveal that the laminar flame speed of cyclopentadiene depends notably on several fuel specific reactions. The role of cyclopentadienyl radical is mainly governed by its formation via H-abstraction reactions on CPD by H and OH radicals and its consumption via the H recombination reaction. All these three reactions have a negative effect on the flame speed. On the contrary, as already discussed by Ji et al. [58], different recombination and dismutation reactions of CPDyl radical, with small radicals including CH_3, HO_2 and mainly OH, have a positive effect on the laminar flame speed.

5. Conclusions

The thermal decomposition of 1,3-cyclopentadiene (CPD) has been studied both experimentally and computationally. A set of new experimental data, obtained for high partial pressures of CPD and the CPD-yl radical, that can be used for model validation is presented and discussed. The experimental work has been performed in a tubular continuous flow pyrolysis reactor under atmospheric pressure and varying nitrogen dilutions, covering a temperature range from 873 to 1123 K. Under the most severe conditions $T > 1120$ K and $\delta = 5$ mol_{N2}/mol_{CPD}), up to 84% of CPD is converted into products, and the amount of PAHs in the effluent is above 65 wt%. Major products observed during CPD pyrolysis in both dilution regimes are benzene, indene and naphthalene, as well as heavier PAHs. The amount of PAHs increases linearly with the conversion of CPD, indicating that the CPDyl radical and its corresponding 1,3-cyclopentadiene play an important role in PAHs formation. These data further contribute to refine an existing detailed kinetic mechanism for pyrolysis and combustion of hydrocarbon and renewable fuels. The data and model predictions are also compared with other pyrolysis and combustion datasets of CPD such as premixed laminar flame speed measurements to further extend the validity of the kinetic model in oxidation conditions. The results obtained with the developed mechanism are in good agreement with the new and existing experimental observations.

Acknowledgments

The research leading to these results has received funding from the Long Term Structural Methusalem Funding by the Flemish Government. The work at Politecnico di Milano was supported by the PRIN 08 (Soot Project). The Authors also gratefully acknowledge the useful discussion with Prof. Mario Dente and Tiziano Faravelli.

Appendix A. Supplementary material

Supplementary data associated with this article can be found, in the online version.

References

[1] C.F. Melius, M.E. Colvin, N.M. Marinov, W.J. Pitz, S.M. Senkan, Sympo. (Int.) Combus. 26 (1) (1996) 685–692, http://dx.doi.org/10.1016/S0082-0784(96)80276-1.
[2] J.A. Mulholland, M. Lu, D.-H. Kim, Proc. Combust. Inst. 28 (2) (2000) 2593–2599, http://dx.doi.org/10.1016/S0082-0784(00)80677-3.
[3] D.H. Kim, J.A. Mulholland, D. Wang, A. Violi, J. Phys. Chem. A 114 (47) (2010) 12411–12416, http://dx.doi.org/10.1021/jp106749k.
[4] M. Szwarc, Chem. Rev. 47 (1) (1950) 75–173, http://dx.doi.org/10.1021/cr60146a002.
[5] R. Spielmann, C.A. Cramers, Chromatographia 5 (12) (1972) 295–300, http://dx.doi.org/10.1007/BF02310746.
[6] R. Cypres, B. Bettens, Tetrahedron 30 (10) (1974) 1253–1260. <http://dx.doi.org/10.1016/S0040-4020(01)97298-9>.
[7] R. Cypres, B. Bettens, Tetrahedron 31 (4) (1975) 359–365. <http://dx.doi.org/10.1016/0040-4020(75)80046-9>.
[8] J.A. Manion, R. Louw, J. Phys. Chem. 93 (9) (1989) 3563–3574, http://dx.doi.org/10.1021/j100346a040.
[9] N.M. Marinov, W.J. Pitz, C.K. Westbrook, M.J. Castaldi, S.M. Senkan, Combust. Sci. Technol. 116–117 (1–6) (1996) 211–287, http://dx.doi.org/10.1080/00102209608935550.
[10] M. Frenklach, J. Warnatz, Combust. Sci. Technol. 51 (4–6) (1987) 265–283, http://dx.doi.org/10.1080/00102208708960325.
[11] M. Frenklach, H. Wang, in: H. Bockhorn (Ed.), Soot Formation in Combustion, vol. 59, Springer, Berlin, Heidelberg, 1994, pp. 165–192.
[12] M. Frenklach, Phys. Chem. Chem. Phys. 4 (11) (2002) 2028–2037.
[13] H. Richter, J.B. Howard, Prog. Energy Combust. Sci. 26 (4–6) (2000) 565–608. <http://dx.doi.org/10.1016/S0360-1285(00)00009-5>.
[14] H. Wang, Proc. Combust. Inst. 33 (1) (2011) 41–67. <http://dx.doi.org/10.1016/j.proci.2010.09.009>.
[15] A. D'Anna, Energy Fuels 22 (3) (2008) 1610–1619, http://dx.doi.org/10.1021/ef700641u.
[16] D. Wang, A. Violi, D.H. Kim, J.A. Mullholland, J. Phys. Chem. A 110 (14) (2006) 4719–4725, http://dx.doi.org/10.1021/jp053628a.
[17] M.B. Colket, D.J. Seery, Sympos. (Int.) Combust. 25 (1) (1994) 883–891, http://dx.doi.org/10.1016/S0082-0784(06)80723-X.
[18] K. Hemelsoet, V. Van Speybroeck, K.M. Van Geem, G.B. Marin, M. Waroquier, Mol. Simul. 34 (2) (2008) 193–199, http://dx.doi.org/10.1080/08927020801930588.
[19] V. Van Speybroeck, M.-F. Reyniers, G.B. Marin, M. Waroquier, ChemPhysChem 3 (10) (2002) 863–870 (10.1002/1439-7641(20021018)3:10<863::AID-CPHC863>3.0.CO;2-P).
[20] H. Richter, T.G. Benish, O.A. Mazyar, W.H. Green, J.B. Howard, Proc. Combust. Inst. 28 (2) (2000) 2609–2618, http://dx.doi.org/10.1016/S0082-0784(00)80679-7.
[21] V.V. Kislov, A.M. Mebel, J. Aguilera-Iparraguirre, W.H. Green, J. Phys. Chem. A 116 (16) (2012) 4176–4191, http://dx.doi.org/10.1021/jp212338g.
[22] S. Sharma, W.H. Green, J. Phys. Chem. A 113 (31) (2009) 8871–8882, http://dx.doi.org/10.1021/jp900679t.
[23] V.V. Kislov, A.M. Mebel, J. Phys. Chem. A 112 (4) (2008) 700–716, http://dx.doi.org/10.1021/jp077493f.
[24] R.D. Kern, Q. Zhang, J. Yao, B.S. Jursic, R.S. Tranter, M.A. Greybill, J.H. Kiefer, Sympos. (Int.) Combust. 27 (1) (1998) 143–150, http://dx.doi.org/10.1016/S0082-0784(98)80399-8.
[25] K. Roy, C. Horn, P. Frank, V.G. Slutsky, T. Just, Sympos. (Int.) Combust. 27 (1) (1998) 329–336. <http://dx.doi.org/10.1016/S0082-0784(98)80420-7>.
[26] V.V. Kislov, A.M. Mebel, J. Phys. Chem. A 111 (38) (2007) 9532–9543, http://dx.doi.org/10.1021/jp0732099.
[27] C. Cavallotti, D. Polino, A. Frassoldati, E. Ranzi, J. Phys. Chem. A 116 (13) (2012) 3313–3324, http://dx.doi.org/10.1021/jp212151p.
[28] C. Cavallotti, S. Fascella, R. Rota, S. Carrà, Combust. Sci. Technol. 176 (5–6) (2004) 705–720, http://dx.doi.org/10.1080/00102200490428026.
[29] H. Ismail, J. Park, B.M. Wong, W.H. Green Jr., M.C. Lin, Proc. Combust. Inst. 30 (1) (2005) 1049–1056. <http://dx.doi.org/10.1016/j.proci.2004.08.127>.
[30] V.V. Kislov, A.M. Mebel, J. Phys. Chem. A 111 (19) (2007) 3922–3931, http://dx.doi.org/10.1021/jp067135x.
[31] S. Fascella, C. Cavallotti, R. Rota, S. Carrà, J. Phys. Chem. A 109 (33) (2005) 7546–7557, http://dx.doi.org/10.1021/jp051508x.
[32] G. Da Silva, J.W. Bozzelli, J. Phys. Chem. A 113 (44) (2009) 12045–12048, http://dx.doi.org/10.1021/jp907230b.
[33] A. Matsugi, A. Miyoshi, Int. J. Chem. Kinet. 44 (3) (2012) 206–218, http://dx.doi.org/10.1002/kin.20625.
[34] R.G. Butler, I. Glassman, Proc. Combust. Inst. 32 (1) (2009) 395–402. <http://dx.doi.org/10.1016/j.proci.2008.05.010>.
[35] S. Granata, F. Cambianica, S. Zinesi, T. Faravelli, E. Ranzi. in: Detailed Kinetics of PAH and Soot Formation in Combustion Processes: Analogies and Similarities

in Reaction Classes, European Combustion Symposium, Louvain-La-Neuve, 2005; Louvain-La-Neuve, 2005.
[36] M. Djokic, H.-H. Carstensen, K.M. Van Geem, G.B. Marin, Proc. Combust. Inst. 34 (1) (2013) 251–258. <http://dx.doi.org/10.1016/j.proci.2012.05.066>.
[37] S.P. Pyl, C.M. Schietekat, K.M. Van Geem, M.-F. Reyniers, J. Vercammen, J. Beens, G.B. Marin, J. Chromatogr. A 1218 (21) (2011) 3217–3223, http://dx.doi.org/10.1016/j.chroma.2010.12.109.
[38] S.P. Pyl, K.M. Van Geem, P. Puimège, M.K. Sabbe, M.-F. Reyniers, G.B. Marin, Energy 43 (1) (2012) 146–160. <http://dx.doi.org/10.1016/j.energy.2011.11.032>.
[39] J. Beens, H. Boelens, R. Tijssen, J. Blomberg, J. High Resolut. Chromatogr. 21 (1) (1998) 47–54, http://dx.doi.org/10.1002/(sici)1521-4168(19980101)21:1<47::aid-jhrc47>3.0.co;2-5.
[40] D. Manca, G. Buzzi-ferraris, T. Faravelli, E. Ranzi, Combust. Theor. Model. 5 (2) (2001) 185–199, http://dx.doi.org/10.1088/1364-7830/5/2/304.
[41] A. Cuoci, A. Frassoldati, T. Faravelli, E. Ranzi, in: OpenSMOKE: Numerical modeling of reacting systems with detailed kinetic mechanisms, XXXIV Meeting of the Italian Section of the Combustion Institute, Rome (Italy), 2011; Rome (Italy), 2011.
[42] E. Ranzi, Energy Fuels 20 (3) (2006) 1024–1032, http://dx.doi.org/10.1021/ef060028h.
[43] E. Ranzi, A. Frassoldati, R. Grana, A. Cuoci, T. Faravelli, A.P. Kelley, C.K. Law, Prog. Energy Combust. Sci. 38 (4) (2012) 468–501, http://dx.doi.org/10.1016/j.pecs.2012.03.004.
[44] E. Ranzi, M. Dente, T. Faravelli, G. Pennati, Combust. Sci. Technol. 95 (1–6) (1993) 1–50, http://dx.doi.org/10.1080/00102209408935325.
[45] R.J. Kee, J.A. Miller, F.M. Rupley, U.S.D.o. Energy, S.N. Laboratories, The Chemkin Thermodynamic Data Base, Micromedia Limited, 1990.
[46] E. Goos, A. Burcat, B. Ruscic, in: <http://garfield.chem.elte.hu/Burcat/burcat.html>, 2013.
[47] S.W. Benson, Thermochemical Kinetics: Methods for the Estimation of Thermochemical Data and Rate Parameters, Wiley, 1976.
[48] E.R. Ritter, J.W. Bozzelli, Int. J. Chem. Kinet. 23 (9) (1991) 767–778, http://dx.doi.org/10.1002/kin.550230903.
[49] A.L. Lafleur, J.B. Howard, K. Taghizadeh, E.F. Plummer, L.T. Scott, A. Necula, K.C. Swallow, J. Phys. Chem. 100 (43) (1996) 17421–17428, http://dx.doi.org/10.1021/jp9605313.
[50] E. Heckmann, H. Hippler, J. Troe, Sympos. (Int.) Combust. 26 (1) (1996) 543–550. <http://dx.doi.org/10.1016/S0082-0784(96)80258-X>.
[51] A.D'. Anna, M. Sirignano, J. Kent, Combust. Flame 157 (11) (2010) 2106–2115. <http://dx.doi.org/10.1016/j.combustflame.2010.04.019>.
[52] C. Cavallotti, D. Polino, Proc. Combust. Inst. 34 (1) (2013) 557–564. <http://dx.doi.org/10.1016/j.proci.2012.05.097>.
[53] R.K. Robinson, R.P. Lindstedt, Combust. Flame 158 (4) (2011) 666–686. <http://dx.doi.org/10.1016/j.combustflame.2010.12.001>.
[54] N.A. Slavinskaya, M. Braun-Unkhoff, P. Frank, in: Modeling of PAH and Polyyne Formation in Premixed Atmospheric Flames C_2H_4/Air, European Combustion Symposium, Louvain-La-Nueve, 2005; Louvain-La-Nueve, 2005.
[55] J. Appel, H. Bockhorn, M. Frenklach, Combust. Flame 121 (1-2) (2000) 122–136. <http://dx.doi.org/10.1016/S0010-2180(99)00135-2>.
[56] A. Fahr, S.E. Stein, Sympos. (Int.) Combust. 22 (1) (1989) 1023–1029, http://dx.doi.org/10.1016/S0082-0784(89)80112-2.
[57] M.G. Brioukov, J. Park, M.C. Lin, Int. J. Chem. Kinet. 31 (8) (1999) 577–582, http://dx.doi.org/10.1002/(SICI)1097-4601(1999) 31:8<577::AID-KIN7>3.0.CO;2-K.
[58] C. Ji, R. Zhao, B. Li, F.N. Egolfopoulos, Proc. Combust. Inst. 34 (1) (2013) 787–794, http://dx.doi.org/10.1016/j.proci.2012.07.047.
[59] Z. Zhao, M. Chaos, A. Kazakov, F.L. Dryer, Int. J. Chem. Kinet. 40 (1) (2008) 1–18, http://dx.doi.org/10.1002/kin.20285.